Robust Missile Autopilot Design using Dynamic Inversion and PI Control

Sungjin Cho, Seung-Hwan Kim, Dong-Gyun Choe

Agency for Defense Development, P.O. Box 35-3, Yuseong, Daejeon, 305-600, Republic of Korea

Abstract: This paper presents a robust nonlinear autopilot design method based on dynamic inversion and PI control law. The new controller structure which is different from previous work is composed of classical linear PI control law and nonlinear fast dynamic inversion. A pitch-axis model of highly maneuverable missiles and a linearized model for designing PI controller are presented. The performance of proposed method is illustrated via nonlinear simulations including aerodynamic uncertainties and actuator dynamics.

Keywords: Missiles, Flight Control, Nonlinear Control, Dynamic Inversion, Robustness

1. Introduction

Dynamic inversion based on feedback linearization is employed to design nonlinear autopilot for a highly maneuverable missile. The dynamic inversion controller has excellent performance due to containing basic concept which is to cancel out the plant's natural dynamics. Several methods have been studied in aircraft or missiles with highly nonlinear characteristics (Snell, *et al.*, 1992; Schumacher and Khargonekar, 1997; Schumacher and Khargonekar, 1998).

However, in spite of such advantage, the control input derived from this method does not perfectly cancel system dynamics because of uncertainty in aerodynamic forces and moments (Steinicke and Michalka, 2002). Also, system's performance and robustness are not guaranteed by the limitation of actuator's dynamics. In order to overcome these difficulties, the various methods combining nonlinear dynamic inversion with stabilizing linear controller can be found in (Escande, 1998; McFarland, *et al.*, 1994; Menon, *et al.*, 1997; McFarland, *et al.*, 2000; Steinicke and Michalka, 2002). Especially, the results in (Menon, *et al.*, 1997; McFarland, *et al.*, 2000; Steinicke and Michalka, 2002) show that PI controller which stabilizes closed loop is included for outer loop design of dynamic inversion.

In this paper, a new robust autopilot design methodology using dynamic inversion and classical PI control law is presented. The proposed autopilot includes nonlinear fast dynamic inversion controller and linear PI controller without slow dynamic inversion controller. The advantage of this method has more robust than previous work including both fast dynamic inversion and slow dynamic inversion. Moreover, tedious work to design traditional gain scheduling controller for inner loop can be partially avoided.

The paper is organized as follows. Firstly, a nonlinear missile model and linearized model as well as actuator dynamics model are described. Secondly, three nonlinear autopilot design methods, i.e. dynamic inversion method, dynamic inversion method with PI control law and proposed method, are presented. The next section contains nonlinear simulation results about three methods. Finally, some conclusions are provided in the last section.

2. Nonlinear Missile Model and Linearized Model

Nonlinear missile model considered in this paper can be found in (Hull and Qu, 1997; Nichols, *et al*., 1993; Reichert, 1992; Shamma and Cloutier, 1993). This model provides a common basis for developing and understanding new approaches to the missile controller problem (Hull and Qu, 1997). The model

consists of pitch-axis force and moment equations which is representative of a generic missile travelling at Mach 3 at an altitude of 20,000 ft and with aerodynamic coefficients represented as third order polynomials in angle of attack. The nonlinear missile dynamics model is described by

$$\dot{\alpha}(t) = f_{r2d} K_\alpha M C_n(\alpha(t), \delta(t), M) \cos(\alpha(t) / f_{r2d}) + q(t) \quad (1)$$

$$\dot{q}(t) = f_{r2d} K_q M^2 C_m(\alpha(t), \delta(t), M) \quad (2)$$

The various plant variables are defined by

$\alpha(t)$: angle of attack(deg), $q(t)$: pitch rate(deg/s)

$P_0 = 973.7\, lbf / ft^2$ (static pressure at 20,000 ft)

$S = 0.44\, ft^2$ (surface area)

$m = 13.98\, slugs$ (mass)

$v_s = 1364.4\, ft/s$ (speed of sound at 20,000ft)

$d = 0.75\, ft$ (diameter)

$M = 3$ (Mach number)

$I_y = 182.5\, slug \cdot ft^2$ (pitch moment of inertia)

$f_{r2d} = \dfrac{180}{\pi}$ (rad-to-degree)

$K_\alpha = \dfrac{0.7 P_0 S}{m v_s}$, $K_q = \dfrac{0.7 P_0 S d}{I_y}$

The aerodynamic coefficients of normal force and pitch moment are approximated by

$$C_n(\alpha(t), \delta(t), M) = \phi_n(\alpha(t)) + d_n \delta(t) \quad (3)$$

$$C_m(\alpha(t), \delta(t), M) = \phi_m(\alpha(t)) + d_m \delta(t) \quad (4)$$

$$\phi_n(\alpha(t)) = \mathrm{sgn}(\alpha)[a_n |\alpha(t)|^3 + b_n |\alpha(t)|^2 + c_n(2 - M/3)|\alpha(t)|] + d_n \delta(t) \quad (5)$$

$$\phi_m(\alpha(t)) = \mathrm{sgn}(\alpha)[a_m |\alpha(t)|^3 + b_m |\alpha(t)|^2 + c_m(-7 + 8M/3)|\alpha(t)|] + d_m \delta(t) \quad (6)$$

These approximations are valid for α in the range of ± 20 degrees. The nonlinear state equations (1) and (2) are linearized about trim operating points ($M_y = 0$) to form linear state-space equations. Linearized equations are as follows.

$$\Delta\dot{\alpha}(t) = \frac{\partial F_z}{\partial \alpha}\Delta\alpha + \frac{\partial F_z}{\partial \delta}\Delta\delta + \frac{\partial F_z}{\partial q}\Delta q \quad (7)$$

$$\Delta\dot{q}(t) = \frac{\partial M_y}{\partial \alpha}\Delta\alpha + \frac{\partial M_y}{\partial \delta}\Delta\delta \quad (8)$$

where F_z and M_y mean the right terms of equation (1), (2). The partial derivatives of equation (7), (8) are given by

$$\frac{\partial F_z}{\partial \alpha} = f_{r2d} K_\alpha M \left\{ \frac{\partial C_n}{\partial \alpha}\cos\alpha + \frac{\partial(\cos\alpha)}{\partial \alpha} C_n \right\}_{\alpha_0\, \delta_0}$$

$$\frac{\partial F_z}{\partial \delta} = f_{r2d} K_\alpha M \left\{ \frac{\partial C_n}{\partial \delta}\cos\alpha \right\}_{\alpha_0\, \delta_0} \quad (9)$$

$$\frac{\partial F_z}{\partial q} = 1,\ \frac{\partial M_y}{\partial \alpha} = f_{r2d} K_q M \left\{ \frac{\partial C_m}{\partial \alpha} \right\}_{\alpha_0\, \delta_0}$$

$$\frac{\partial M_y}{\partial \delta} = f_{r2d} K_q M \left\{ \frac{\partial C_m}{\partial \delta} \right\}_{\alpha_0\, \delta_0}$$

Linearized state equations are obtained by arranging equations (7), (8)

$$\begin{bmatrix} \dot{\alpha} \\ \dot{q} \end{bmatrix} = \begin{bmatrix} Z_\alpha & 1 \\ M_\alpha & 0 \end{bmatrix} \begin{bmatrix} \alpha \\ q \end{bmatrix} + \begin{bmatrix} Z_\delta \\ M_\delta \end{bmatrix} \delta \quad (10)$$

where the dimensional derivatives are defined by

$$Z_\alpha = \frac{\partial F_z}{\partial \alpha},\ Z_\delta = \frac{\partial F_z}{\partial \delta},\ Z_q = 1,\ M_\alpha = \frac{\partial M_y}{\partial \alpha},\ M_\delta = \frac{\partial M_y}{\partial \delta}$$

The tail fin actuator's model can be presented by the 2nd order transfer functions.

$$\frac{\delta_p}{\delta_c} = \frac{\omega_n^2}{s^2 + 2\varsigma\omega_n s + \omega_n^2} \quad (11)$$

where

δ_c = commanded fin deflection, deg

ς =2nd order actuator damping ratio, 0.7

ω_n =2nd order actuator bandwidth, 20Hz

In this study, slew rate and saturation limit are considered for practical research. Slew rate limit causes the change of actuator's bandwidth and damping ratio. Also, saturation limit, i.e. mechanical limit of actuator, restricts enough control power. The limit value of tail fin deflection is $\pm$ 50 degree. This value results from (Hull and Qu, 1997). And, slew rate limit value is $\pm$ 300 deg/s.

3. Nonlinear Autopilot Design Methods

3.1 Nonlinear Dynamic Inversion

The first design methodology used in this paper is a dynamic inversion approach using a two time scale assumption. The method can be found in (Snell, *et al.*, 1992). The controller structure is shown in Fig. 1

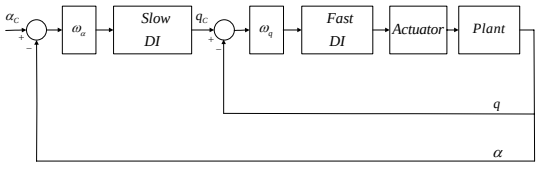

Fig. 1. The structure of dynamic inversion controller

The inner loop of the dynamic inversion control law controls the "fast state" q. This loop calculates tail fin commands from the rate commands q_C given by the slow inversion in Fig. 1. The desired dynamics for the inner loop are given by $\dot{q}_d = \omega_q(q_C - q)$ where ω_q is 3Hz. A slow inversion is applied to the dynamics of the "slow state" α . The slow inversion attempts to replace the actual alpha dynamics with the desired dynamics $\dot{\alpha}_d = \omega_\alpha(\alpha_C - \alpha)$ where ω_α is 1Hz. The inversion control law has the following form.

$$q_c = \dot{\alpha}_d - K_\alpha M \cos(\alpha(t)/f_{r2d})\{\phi_n(\alpha(t)) + d_n\delta(t)\} \quad (12)$$

$$\delta_c = \frac{1}{K_q M^2 d_m}\{\dot{q}_d - K_q M^2 \phi_m(\alpha(t))\} \quad (13)$$

3.2 Nonlinear Dynamic Inversion with PI control

The second design methodology used in this paper is a dynamic inversion with PI control law. This method is similar to (Menon, *et al.*, 1997; McFarland, *et al.*, 2000; Steinicke and Michalka, 2002). The controller structure is shown in Fig. 2.

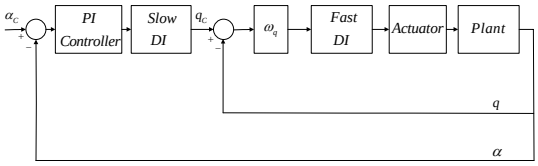

Fig. 2. The structure of dynamic inversion controller with PI controller

The characteristics of the method have classical PI controller considered as outer loop of dynamic inversion. The role of PI controller is to stabilize the closed loop for uncertainty. To form the closed loop transfer functions, the equation related to PI gain is derived from

$$\dot{\alpha}_d \cong \dot{\alpha} = K_P(\alpha_c - \alpha) + K_I \int_0^t (\alpha_c - \alpha) d\tau \quad (14)$$

Therefore, the transfer function consists of PI gain without aerodynamic property as follows.

$$\frac{\alpha}{\alpha_c} = \frac{K_p s + K_I}{s^2 + K_P s + K_I} \quad (15)$$

In equation (15), PI gains K_p, K_I are decided to satisfy 1Hz of closed loop bandwidth and less 5% of percent overshoot by using pole placement technique. This means the performance of this method is similar to that of the first design method in nominal case.

3.3 A Proposed Controller: Fast Dynamic Inversion with PI control

In this paper, new methodology for robust autopilot design is to use fast dynamic inversion and PI control law. The controller structure is shown in Fig. 3.

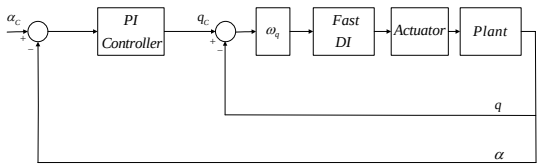

Fig. 3. The structure of a new robust nonlinear controller

From the new method, we obtain fast response for uncertainty rather than the design methods of section 3.1 and 3.2. In addition, tedious work to design traditional gain scheduling controller for inner loop can be partially avoided through the method. For the purpose of designing PI controller, the closed loop system including linearized plant is described by Fig. 4.

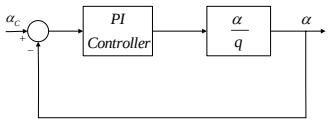

Fig. 4. Closed loop system for PI controller design

The transfer function of the linearized plant is derived from equation (10) as follows.

$$\frac{\alpha}{q} = \frac{Z_\delta s + M_\delta}{M_\delta s + (M_\alpha Z_\delta - Z_\alpha M_\delta)} \quad (16)$$

The proposed PI controller has the following form.

$$q_C \cong q = K_P(\alpha_c - \alpha) + K_I \int_0^t (\alpha_c - \alpha) d\tau \quad (17)$$

Dimensional derivatives Z_α, M_α, Z_δ, M_δ are the value for trim α, δ. In this study, trim α, δ are both zeros. PI gains K_P, K_I are selected to satisfy 1Hz of closed loop bandwidth and less 5% of percent overshoot by using root locus technique.

4. Nonlinear Simulations

For nonlinear simulation, angle of attack command is considered as various magnitudes such as 5, 10 and 20 degrees. Simulation results without aerodynamic uncertainty are in Fig. 5. In nominal case, the performance of dynamic inversion controller is better than that of new robust nonlinear controller in the view of percent overshoot and settling time. Also, the control input of dynamic inversion controller is less than those of two controllers.

Nonlinear simulations are performed to check robustness of controller when aerodynamic uncertainty is ± 20%. Simulation results with -20% of aerodynamic uncertainty are in Fig. 6. In this case, nonlinear dynamic inversion controller does not follow the angle of attack command and makes control input stay the limit of tail fin deflection angle. And nonlinear dynamic inversion controller with PI control law results in oscillation of angle of attack response. However, in the proposed controller, tracking performance is remarkably improved in spite of aerodynamic uncertainty -20%, and control energy is relatively minimized.

In case of aerodynamic uncertainty +20%, simulation results are in Fig. 7. From these results, new design method can reduces the steady state error faster than nonlinear dynamic inversion with PI control law.

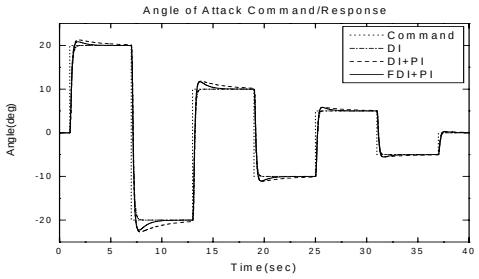

(a) Alpha command vs. response

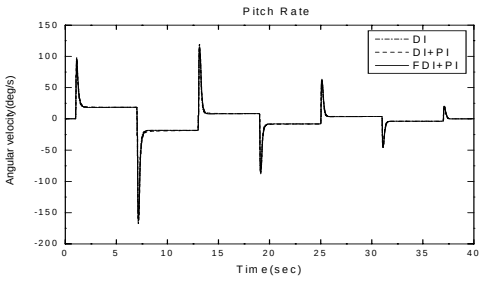

(b) Pitch rate response

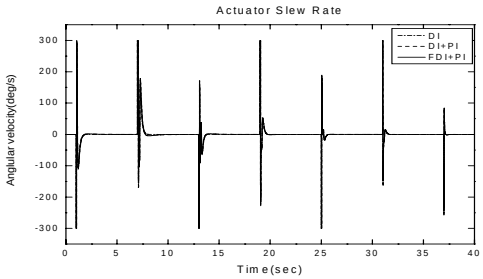

(c) Actuator's slew rate

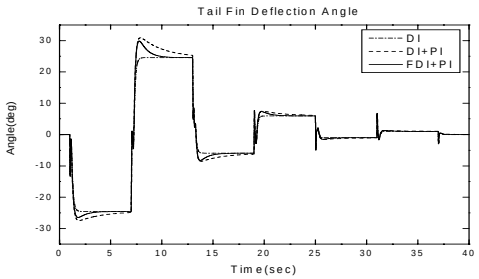

(d) Tail fin deflection angle

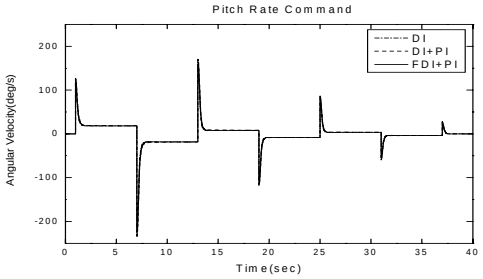

(e) Pitch rate command

Fig. 5. Simulation results (nominal case): dotted, command; dash dotted, DI(dynamic inversion controller); dashed, DI+PI(dynamic inversion controller with PI controller); solid, FDI+PI(a proposed controller)

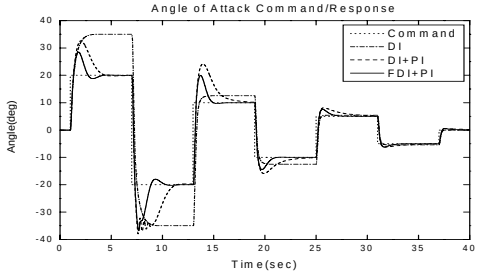

(a) Alpha command vs. response

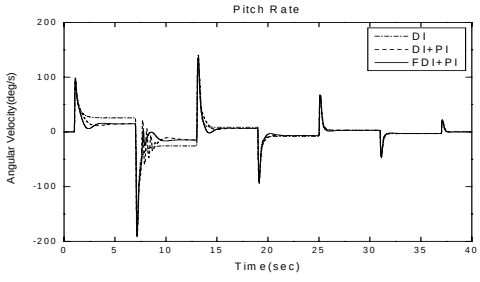

(b) Pitch rate response

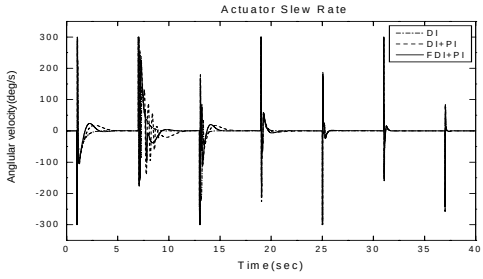

(c) Actuator's slew rate

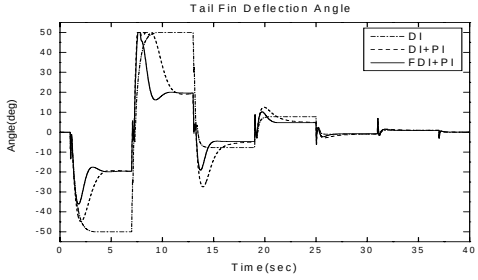

(d) Tail fin deflection angle

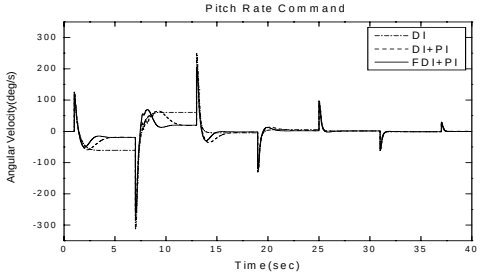

(e) Pitch rate command

Fig. 6. Simulation results (uncertainty case (-20%)): dotted, command; dash dotted, DI(dynamic inversion controller); dashed, DI+PI(dynamic inversion controller with PI controller); solid, FDI+PI(a proposed controller)

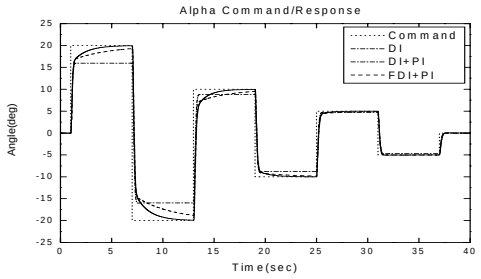

(a) Alpha command vs. response

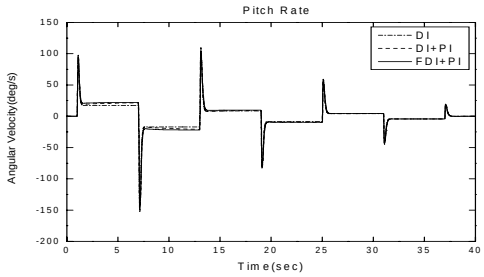

(b) Pitch rate response

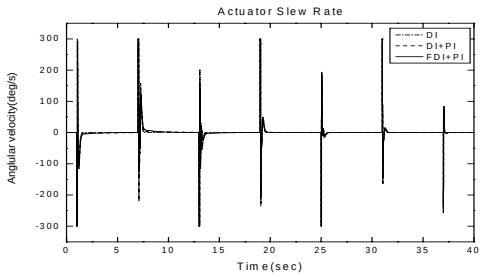

(c) Actuator's slew rate

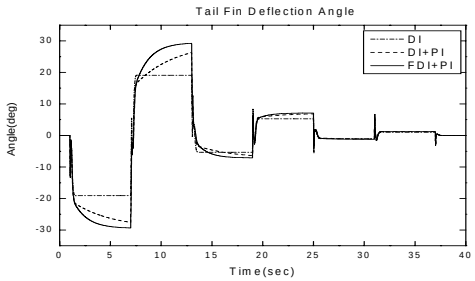

(d) Tail fin deflection angle

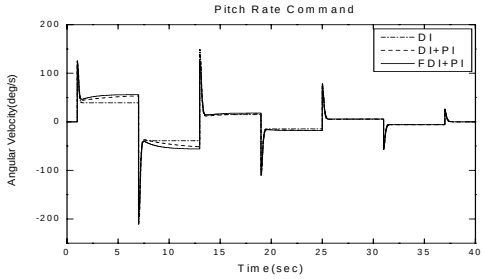

(e) Pitch rate command

Fig. 7. Simulation results (uncertainty case (+20%)): dotted, command; dash dotted, DI(dynamic inversion controller); dashed, DI+PI(dynamic inversion controller with PI controller); solid, FDI+PI(a proposed controller)

5. Conclusion

Robust nonlinear controller structure proposed in this paper illustrates that tracking performance is superior to that of two previous nonlinear controller when aerodynamic uncertainty exists. Nonlinear dynamic inversion controller does not follow the angle of attack command and makes control input stay the limit of tail fin deflection angle owing to aerodynamic uncertainties and actuator dynamics' limitation. And, nonlinear dynamic inversion controller with PI control law results in oscillation of angle of attack response in case of aerodynamic uncertainty -20%. The proposed controller shows good tracking performance through minimization of control energy.

Further study will aim at stability analysis and performance confirmation through the 6-DOF simulation.

REFERENCES

Escande, B. (1998).
Nonlinear Dynamic Inversion and Linear Quadratic Techniques. *AIAA Guidance, Navigation, and Control Conference and Exhibit*, AIAA-1998-4245.

Hull, R. A. and Z. Qu (1997).
Dynamic Robust Recursive Control Design and Its Application to a Nonlinear Missile Autopilot. *Proc. of the American Control Conference*, pp. 833-837.

Menon, P. K., V. R. Iragavarapu and E. J. Ohlmeyer(1997).
Nonlinear Missile Autopilot Design using Time-Scale Separation. *AIAA Guidance, Navigation, and Control Conference and Exhibit*, AIAA-1997-3765.

McFarland, M. B. and C. N. D'Souza (1994).
Missile Autopilot Design using Dynamic Inversion and Structured Singular Value Synthesis. *Proc. of the American Control Conference*, pp. 959-961.

McFarland, M. B. and S. M. Hoque (2000).
Robustness of a Nonlinear Missile Autopilot Designed using Dynamic Inversion. *AIAA Guidance, Navigation, and Control Conference and Exhibit*, AIAA-2000-3970.

Nichols, R. A., R. T. Reichert and W. J. Rugh (1993).
Gain Scheduling for H-Infinity Controllers: A Flight Control Example. *IEEE Trans. On Control Systems Technology*, **Vol. 1**, **No. 2**, pp. 69-79.

Reichert, R. (1992).
Dynamic Scheduling of Modern-Robust-Control Autopilot Designs for Missiles. *IEEE Control Systems Magazine*, **Vol. 12**, **No. 5**, pp. 35-42.

Schumacher C. and P. P. Khargonekar (1997).
A Comparison of Missle Autopilot Design using H-Infinity Control with Gain Scheduling and Nonlinear Dynamic Inversion. *Proc. of the American Control Conference*, pp. 2759-2763.

Schumacher C. and P. P. Khargonekar (1998).

Stability Analysis of a Missile Control System with a Dynamic Inversion Controller. *Journal of Guidance, Control, and Dynamics,* **Vol. 21**, **No. 3**, pp. 508-515.

Shamma, J. S. and J. R. Cloutier (1993). Gain-Scheduled Missile Autopilot Design Using Linear Parameter Varying Transformation. *Journal of Guidance, Control, and Dynamics,* **Vol. 16, No. 2**, pp. 256-263.

Snell, S., A., D. F. Enns and W. L. Garrard (1992). Nonlinear Inversion Flight Control for a Supermaneuverable Aircraft. *Journal of Guidance, Control, and Dynamics,* **Vol. 15**, **No. 4**, pp. 976-984.

Steinicke, A. and G. Michalka (2002). Improving Transient Performance of Dynamic Inversion Missile Autopilot by Use of Backstepping. *AIAA Guidance, Navigation, and Control Conference and Exhibit,* AIAA-2002-4658.

Steinberg, M. L. (1999). A Comparion of Intelligent, Adaptive, and Nonlinear Flight Control Laws. *AIAA Guidance, Navigation, and Control Conference and Exhibit,* AIAA-1999-4044.